I&EC research
Industrial & Engineering Chemistry Research
pubs.acs.org/IECR
Article

CO_2-Tolerant Cryogenic Nitrogen Rejection Schemes: Analysis of Their Performances

Elvira Spatolisano* and Laura A. Pellegrini

Cite This: *Ind. Eng. Chem. Res.* 2021, 60, 4420–4429
Read Online
ACCESS | Metrics & More | Article Recommendations

ABSTRACT: In the transition to a sustainable energy future, natural gas is a key player supporting a shift away from coal, where renewables and other nonfossil fuels may not be able to grow sufficiently on their own. The growing importance of natural gas has led to a re-evaluation of the potential of unconventional, stranded, and contaminated gas reserves that were previously considered economically unviable. Among them, nitrogen-rich natural gas feedstocks, which in the past were thought to be a not-so-interesting methane source, are now becoming a considerable fraction of the total treated gas. For this kind of low-quality gases, nitrogen removal is necessary to lower the inert content and to produce a pipeline-quality gas or liquefied natural gas (LNG). Considering the available nitrogen removal technologies, cryogenic nitrogen rejection is nowadays the leading one for large-scale applications, with capacities exceeding 0.5 million standard cubic meters per day (MSCMD), being very flexible regarding the inlet N_2 content. Depending on the feed composition, different nitrogen rejection units (NRUs—i.e., the single-, the double-, and the three-column systems) are available for treating inlet gas mixtures. The aim of the present work is to evaluate the performances of different cryogenic nitrogen rejection schemes through energy and exergy analysis. Specifically, single-column and three-column nitrogen rejection schemes have been considered with various natural gas feed compositions, focusing on the range where different nitrogen removal schemes are applicable. The net-equivalent methane analysis accounts for the amount of methane required to supply the overall process energy demands through specific processes assumed as reference. On the other hand, exergy analysis evaluates the exergy efficiency of each process scheme through a thermodynamically rigorous approach, converting energy and material flows into their exergy equivalents. Results prove that the three-column process scheme reaches the highest thermodynamic performances, resulting in the best values of exergy efficiency and equivalent methane requirements with respect to the other configurations. This is mainly due to the lower prefractionation column condenser duty, resulting in a less irreversible heat exchanging process.

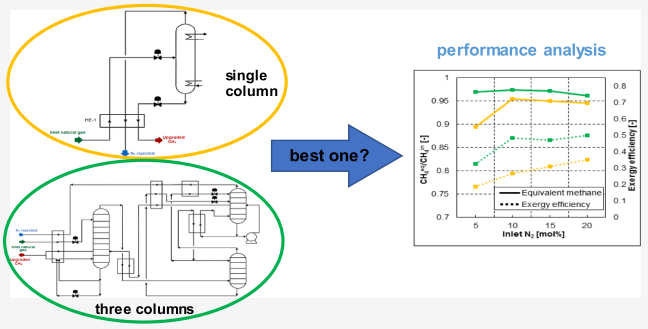

1. INTRODUCTION

The energy sector is currently in the midst of a profound change where technology is revolutionizing the way energy is produced, distributed, and consumed.

Global, European, and national institutions are aware of this deep change and set targets going in the direction of decarbonizing the energy sector. At the international level, the ambitious target established by the COP21 in Paris is setting in motion policymakers worldwide, who are working on policies and measures able to "hold the increase in the global average temperature to well below 2 °C above the preindustrial levels", pursuing efforts to limit the temperature increase to 1.5 °C.[1]

As the energy sector accounts for nearly 90% of CO_2 emissions globally (accounting this percentage for transport, industry, and buildings too), it is the dominant contributor to climate change.[2] For this reason, the world is experiencing a profound energy transition, shifting from an energy system based on fossil fuels to one based on renewable energy.

The Sustainable Development Scenario projected by the International Energy Agency (IEA)[3] maps out a way to meet sustainable energy goals in full, requiring rapid and widespread changes across all parts of the energy system.

According to the International Energy Agency's forecasts, natural gas consumption will increase over the next decade at an annual average rate of 0.9% before reaching a high point by the end of 2020. It is the only source of energy, along with renewables, whose share in primary energy increases over the presented scenario.

Received: December 17, 2020
Revised: February 23, 2021
Accepted: February 23, 2021
Published: March 9, 2021

https://dx.doi.org/10.1021/acs.iecr.0c06189
Ind. Eng. Chem. Res. 2021, 60, 4420–4429

The rise in global requests for natural gas, together with the abundance of unconventional and low-quality reserves, has led to the development of new exploration and production technologies that allow benefiting from fields previously considered economically unviable.

Such low-quality natural gas reserves contain significant concentrations of gases other than methane. These non-hydrocarbons are predominantly nitrogen, carbon dioxide, and hydrogen sulfide, but may also include other gaseous components.

Among these so-called subquality natural gas reserves, nitrogen-rich gases, which in the past were thought to be a not-so-interesting methane source, are now becoming a considerable fraction of the total treated gas. For this kind of low-quality natural gas (whose listing is available in De Guido et al.[4]), deep and technologically challenging purification treatments are necessary to meet sales gas specifications. As subquality fields are exploited, the need for better natural gas upgrading processes is increasing.

Several techniques have been proposed such as cryogenic distillation, membranes, adsorption, and absorption. Nevertheless, cryogenic distillation remains the leading technology for large-scale plants with capacities exceeding 0.5 million standard cubic meters per day (MSCMD), capable of reducing nitrogen to less than 1 mol %, and being very flexible regarding the inlet nitrogen content.[5,6]

Considering cryogenic distillation, different process configurations are available to achieve nitrogen−methane separation, producing a pipeline-quality natural gas. In this context, the aim of this work is to evaluate the performances of different cryogenic nitrogen rejection schemes by comparing them with energy and exergy analyses.

2. CRYOGENIC NITROGEN REJECTION

The cryogenic nitrogen rejection process consists of distillation, where nitrogen and methane are separated exploiting their different volatilities. Due to the very low boiling points of the two species, cryogenic distillation is limited in tolerating impurities in the incoming natural gas feed. Feed gas has to contain mainly methane and nitrogen, and very low quantities of higher hydrocarbons and carbon dioxide are allowed, with the most stringent limit due to the freezing point of the mixture.

Generally, carbon dioxide tolerance is determined by the coldest spot where carbon dioxide tends to freeze. Since the maximum solubility of carbon dioxide depends in essence on the temperature of the solvent, processes at elevated pressure (typically above 20 bar) are more carbon dioxide-tolerant than those operated at low pressure. The main drawback of this process is the high-energy demand because low temperatures are required to fractionate nitrogen and methane mixtures.

Various process configurations can be realized and were simulated in Aspen HYSYS V9.0:[7] single-column process, reported in Figure 1, double-column process, reported in Figure 2, and three-column process, reported in Figure 3.

A description of these schemes is reported in the following, and the details about process simulations are reported elsewhere.[4] The single-column process is typically applied when the nitrogen content in the feed gas is below 30 mol %.[8]

The feed stream, FeedGas, after precooling in LNG-100 against the top and bottom column products, is expanded in VLV-100 and then sent to the distillation column T-100. The column is equipped with a partial reboiler and partial condenser, producing a methane bottom liquid stream CH_4 Product and a

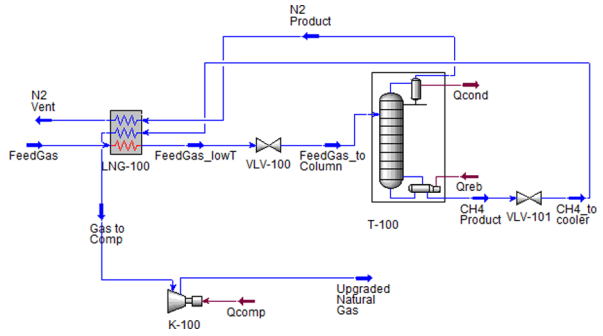

Figure 1. Single-column process scheme simulated in Aspen HYSYS V9.0.

nitrogen top vapor N_2 Product. The bottom product meets sales gas specifications and is suitable, after compression in K-100, to be sent to pipelines, while the nitrogen top product can be either vented (the residue methane content in this stream is of 0.5 mol %, to respect environmental issues[9]) or reinjected into wells for enhanced oil recovery (EOR). The distillation operating pressure is in the range of 21−28 bara, with the process being not viable as the nitrogen critical pressure is approached (about 34 bara).

As the nitrogen content increases, the condensation duty increases, too, and the single-column configuration stops being the most advantageous separation solution. The double column is the preferred choice for nitrogen concentration in the inlet feed above 30 mol %. The double-column process scheme employs two thermally coupled distillation columns, HP_Column, working at high pressure, and LP_Column, working at low pressure. The pressure in the columns is set in such a way that there is an acceptable temperature difference between the thermally linked reboiling and condensing fluids; the high-pressure column operates typically at 10−25 bara, while the low-pressure one at approximately 1.5 bara.[10]

The feed gas, Feed, is first precooled against the two product streams in LNG-100. Exiting from the process−process heat exchanger, it is used to provide duty to the reboiler of the HP_Column, so that it is further cooled down. After expansion in VLV-100, it is fed to the HP_Column, equipped with a partial reboiler and a total condenser. Here, the feed stream is separated into a bottom stream (CH_4_HP), richer in methane, and a top stream (N_2_HP), richer in nitrogen. Both products are fed, after depressurization, to the LP_Column, the former being the feed (CH_4_inLP) and the latter providing the reflux (N_2_inLP). In the LP_Column, separation is completed, and essentially, pure nitrogen and methane are withdrawn at the top (N_2_prod) and at the bottom (CH_4_prod).

The whole process is completely autothermal and does not need any external source for its cooling requirements, entirely fulfilled by internal exchanges (for further details about feed conditions, refer to Section 5). As the high-pressure products are fed to the low-pressure column, where very low temperatures are reached (as low as −190 °C), the process cannot tolerate more than a few ppm of CO_2 because of solidification issues.

The three-column process can be interpreted as a modification of the double-column process. It employs a further upstream distillation column that acts as a high-pressure prefractionator, allowing both to increase the NRU CO_2-tolerance and to concentrate the feed stream processed in the downstream section. The prefractionator, in fact, splits the inlet feed into a bottom stream, richer in the heavy components

https://dx.doi.org/10.1021/acs.iecr.0c06189
Ind. Eng. Chem. Res. 2021, 60, 4420−4429

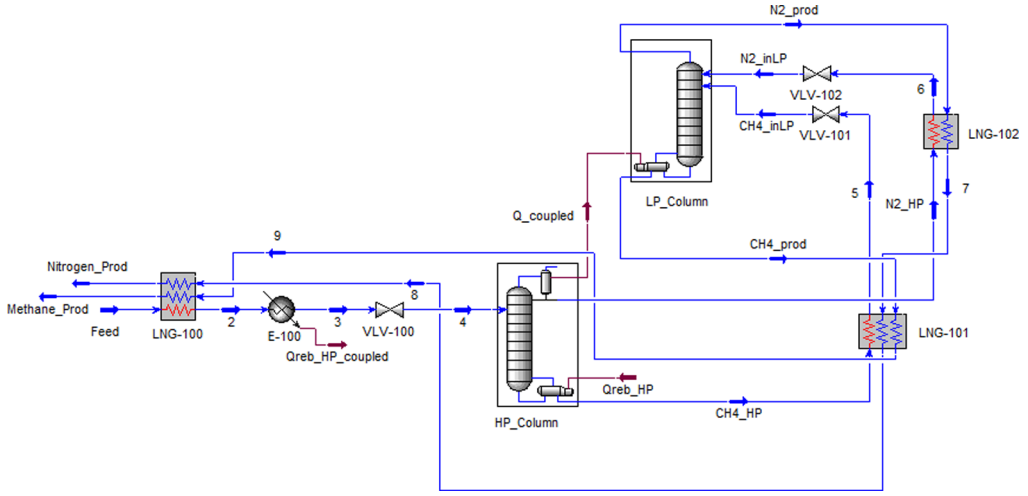

Figure 2. Double-column process scheme simulated in Aspen HYSYS V9.0.

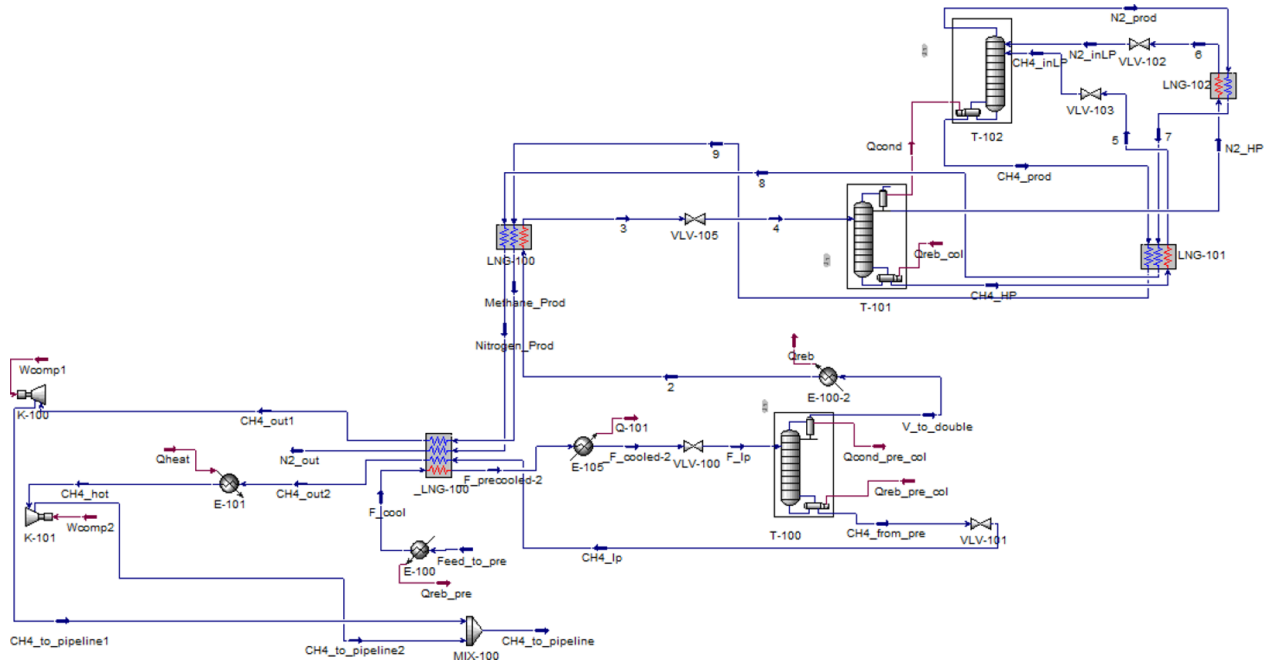

Figure 3. Three-column process scheme simulated in Aspen Plus V9.0.

(methane, carbon dioxide, and higher hydrocarbons) and a top stream, richer in nitrogen. Since its operating pressure is higher, the freezing risks are lowered and higher inlet carbon dioxide concentrations can be tolerated in the overall process.[11−13]

In the three-column process scheme, the feed stream (Feed_to_pre) is used as a heating medium in the reboiler of the preseparation column, simulated as the external heat exchanger E-100. After further cooling against all of the product streams in LNG-100, it is depressurized and sent to the preseparation column T-100. Here, it is fractionated into a concentrated nitrogen vapor stream, V_to_double, sent to the double-column process to complete the separation, and a methane-rich bottom stream, CH_4_from_pre, the pipeline-quality natural gas.

Referring to the schemes reported in Figures 1−3, the feasibility of these different nitrogen rejection schemes in the presence of carbon dioxide was analyzed in a previous work[4] because a CO_2-tolerant NRU may lower the capital and operating costs reducing the upstream CO_2 removal.

The maximum inlet CO_2 content in each of the analyzed configurations is limited by two different constraints: one related to the sales gas specifications in terms of Wobbe index, defined as $\mathrm{WI} = \frac{\mathrm{GCV}}{\sqrt{\rho}}$ (GCV being the gross calorific value and ρ being the specific density), and the other one related to CO_2 solidification within the plant.

Indeed, the maximum-allowable CO_2 content in the feed stream has to guarantee pipeline-quality natural gas production, considering that all of the inlet carbon dioxide is recovered in the upgraded natural gas product. Moreover, CO_2 must not freeze within the plant, so that the CO_2 content might be reduced (with a higher Wobbe index), in principle, after performing a freeze check in the coldest spots of the plant.

Considering only the Wobbe index constraint, the orange line in Figure 4 is obtained: at fixed N_2 inlet feed content, the maximum-allowable CO_2 inlet content was evaluated imposing

https://dx.doi.org/10.1021/acs.iecr.0c06189
Ind. Eng. Chem. Res. 2021, 60, 4420−4429

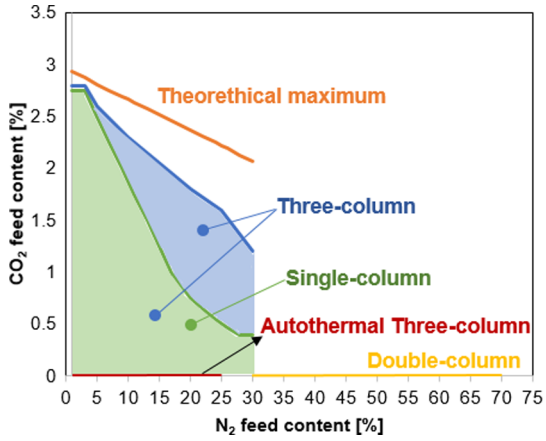

Figure 4. Feasibility analysis of nitrogen rejection schemes.

ideal fractionation (i.e., all N_2 is recovered from the top and all CO_2 and CH_4 are recovered from the bottom of the fractionator).

Starting from this theoretical maximum, a range of applicability was determined for each configuration depending on the N_2 and CO_2 content in the feed gas. At a fixed N_2 inlet fraction, the maximum-allowable CO_2 content in the feed gas was determined as the one suitable to avoid solidification within the process and to permit the methane bottom product reaching the desired value of the Wobbe index. As shown in Figure 4, the stricter constraint is the one for avoiding CO_2 freezing. With reference to Figure 4, two areas can be identified corresponding to the low-nitrogen inlet content (below 30 mol %) and high-nitrogen inlet content (above 30 mol %).

As stated in Mokhatab et al.,[14] the single-column process scheme is industrially applied for the nitrogen feed content below 30 mol %. For the nitrogen feed content higher than 30 mol %, the single-column configuration is still applicable but it is not the preferred one due to the too high condenser thermal load and the too low methane recovery. Considering the high-nitrogen inlet content, only the double column is applicable but no inlet CO_2 is tolerated because of solidification issues: in these situations, a deep CO_2 purification is required upstream of the nitrogen rejection facility. Focusing on the low-nitrogen inlet content, different process schemes can be applied, depending on N_2 and CO_2 concentrations in the feed stream. When the CO_2 feed content is negligible, the autothermicity is achievable for the three-column configuration, maximizing the process−process heat exchange. On the other hand, when the CO_2 feed content is not negligible, both single- and three-column configurations can be used, depending on the specific feed composition. Referring to natural gas feed compositions below the green line in Figure 4, both single- and three-column schemes are applicable. To determine which is the most convenient one between these two, the aim of this work is to assess the performances of these two NRUs, comparing them by means of net-equivalent methane and exergy analyses.

3. PERFORMANCES OF SINGLE- AND THREE-COLUMN NITROGEN REJECTION SCHEMES

Thermodynamic performances of the cryogenic nitrogen rejection schemes (i.e., single- and three-column processes), introduced in Section 2, are assessed by means of energy and exergy analyses.

The energy analysis is performed according to the net-equivalent methane approach,[15,16] while the exergy analysis is performed according to the traditional exergy method, formalized by Kotas[17,18] and Bejan.[19,20]

3.1. Net-Equivalent Methane Analysis. The net-equivalent methane analysis accounts for the amount of methane required by the defined reference processes to deliver thermal and mechanical energies to each one of the analyzed equipment.[13,15] The net energy consumption of the process under study is determined, in this way, as the total net CH_4 amount involved in the process itself.

Going into details, the amount of equivalent methane is equal to the amount of methane produced by the process, plus the amount of methane produced by methane-producing items, minus the amount of methane consumed by the methane-consuming processes (eq 1).

$$\dot{m}_{CH_{4,net}} = \dot{m}_{CH_{4,tot}} + \dot{m}_{CH_{4,produced}} - \dot{m}_{CH_{4,consumed}} \quad (1)$$

In the present case study relevant to the NRU, no methane-producing items are available (see Figures 1−3), while the considered methane-consuming processes are listed as follows.

- Cooling duty produced by a proper refrigeration cycle to cool a process stream down to temperatures lower than the ambient one:

  These refrigeration cycles require mechanical work to be operated, which is considered as electric energy obtained by an equivalent CH_4-fired combined cycle power plant.

  The theoretical ideal coefficient of performance (COP) of the refrigeration cycle can be calculated according to eq 2, where T_H and T_L are the two constant temperatures, respectively, of the condenser and of the evaporator in the refrigeration cycle. The temperature of the hot reservoir is set equal to 25 °C, whereas that of the cold reservoir is determined knowing the outlet temperature of the process stream to be cooled (as obtained from simulations) and considering a temperature approach of 5 °C.

$$COP_{R,Carnot} = \frac{1}{\frac{T_H}{T_L} - 1} \quad (2)$$

  Knowing the theoretical value, the real one can be obtained by:

$$COP_R = COP_{R,Carnot} \cdot \eta_{II} \quad (3)$$

  Evaluating the COP_R, the amount of methane equivalent to the required cooling duty Q can be determined according to:

$$\dot{m}_{CH_4} = \frac{Q}{COP_R \cdot \eta_{CC} \cdot LHV_{CH_4}} \quad (4)$$

- Mechanical work required by compressors: It is evaluated according to eq 5, recalling that the COP_R represents the ratio between the provided cooling duty and the electrical energy consumed, W_{EL}, by the cycle (eq 6).

$$\dot{m}_{CH_4} = \frac{W_{EL}}{\eta_{CC} \cdot LHV_{CH_4}} \quad (5)$$

$$COP_R = \frac{Q}{W_{EL}} \quad (6)$$

https://dx.doi.org/10.1021/acs.iecr.0c06189
Ind. Eng. Chem. Res. 2021, 60, 4420−4429

Table 1 summarizes the values adopted for the lower heating values of methane, the efficiency of the combined cycle (defined according to eq 5), and the second law efficiency (defined as the ratio between the actual thermal efficiency and the maximum (reversible) one at the same conditions) for refrigeration cycles.

Table 1. Parameters Used in the Net-Equivalent CH_4 Analysis

parameter	value	reference
LHV_{CH_4} [MJ/kg]	50	15
η_{CC}	0.55	15
η_{II}	0.60	15

Some energy requirements have not been included in the equivalent methane analysis: reboiler of the distillation column in the single-column process scheme, in which cooling water can be used as the heating medium; reboiler of the HP_column in the double-column process scheme; reboiler of the preseparation column in the three-column process scheme, considering the possibility of energy integration within the process itself (see E-100 in Figures 1 and 3); and reboiler of the LP_column and condenser of the HP_column in the double-column process scheme, which are thermally coupled.

3.2. Exergy Analysis. Exergy expresses the amount of mechanical work necessary to produce a material in its specified state from components common in the natural environment, in a reversible way, heat being exchanged only with the environment.[18]

Exergy analysis allows one to take into account both quantity and quality of energy streams flowing through the control volume boundaries, uniformly expressing them by means of their mechanical energy equivalents. Exergy analysis can be very useful for cryogenic systems, where the temperature level at which thermal energy is provided is of crucial importance, bearing in mind that energy balances treat all forms of energy as equivalent, without differentiating between their different grades crossing the system boundary.

The setup of the exergy balance starts from the definition of the reference environmental conditions. In the following, the reference environment is assumed with a temperature T_0 = 298.15 K and a pressure P_0 = 1.01325 bara and distinguished by the subscript "0".

Fixing the reference state, the exergy efficiency (η_{ex}) can be evaluated, based on the consumed-produced efficiency, which is defined as the ratio between the change in exergy of the treated flows (the actual useful product of the system) and the sum of the external exergy required by the system to perform the desired change,[21] as pointed out in:

$$\eta_{ex} = \frac{\dot{E}x_{out}^{mat} - \dot{E}x_{in}^{mat}}{\dot{E}x^{W} + \dot{E}x^{Q}} \tag{7}$$

The numerator in eq 7 represents the minimum amount of mechanical work required to produce the pipeline-quality natural gas from nitrogen-rich natural gas, i.e., the exergy associated with nitrogen removal processes. The denominator represents the sum of mechanical work and heat duty that must be supplied to the process in order to obtain the desired useful effect.

The exergy associated with the inlet and outlet material streams in the numerator of eq 7 can be evaluated according to eq 8, considering the expressions of physical exergy ($ex_{mixt,i}^{ph}$) and chemical exergy ($ex_{mixt,i}^{Ch}$) reported in eq 9 and eq 10.

$$\dot{E}x^{mat} = \sum_i N_i \cdot (ex_{mixt,i}^{Ph} + ex_{mixt,i}^{Ch}) \tag{8}$$

$$ex_{mixt,i}^{Ph} = h_i - h_{i,0} - T_0 \cdot (s_i - s_{i,0}) \tag{9}$$

$$ex_{mixt,i}^{Ch} = \sum_j (x_{j,i} \cdot ex_{std,j}^{Ch}) + RT_0 \cdot \sum_j [x_{j,i} \ln(x_{j,i})] \tag{10}$$

In eq 9, $h_{i,0}$ and $s_{i,0}$ are, respectively, the molar enthalpy and the molar entropy of each material stream crossing the system boundary, evaluated at the reference temperature T_0 and pressure P_0, while h_i and s_i are the molar enthalpy and entropy of each material stream crossing the system boundary, evaluated at the actual stream temperature T and pressure P.

In eq 10, $x_{j,i}$ stands for the molar fraction of species j in the material stream i, while $ex_{std,j}^{Ch}$ is the standard molar chemical exergy of species j, whose value is reported in Table 2 for each of the considered species.

Table 2. Standard Molar Chemical Exergy for the Species Involved in the Nitrogen Rejection Process

species	$ex_{std,j}^{Ch}$ [kJ/kmol]	references
CH_4	837 000	Szargut, 1962
N_2	720	Szargut, 2005
CO_2	20 189	Szargut, 2005

However, the exergy related to work interactions ($\dot{E}x^{W}$ in eq 7) is numerically equal to the work as energy,[19] as pointed out in eq 11, while the exergy related to heat interactions ($\dot{E}x^{W}$ in eq 7), removed or supplied, can be evaluated from the definition of the Carnot factor, τ_i, which is based on both the temperatures of the environment, T_0, and of the surfaces, T_i, at which the heat transfer of the heat flow Q_i occurs.[19]

$$\dot{E}x^{W} = \sum_i \dot{W}_i$$

$$\dot{E}x^{Q} = \sum_i \dot{Q}_i \cdot \tau_i \tag{11}$$

with $\tau_i = 1 - \frac{T_0}{T_i}$ for $T_i > T_0$

$$\tau_i = \frac{T_0}{T_i} - 1 \text{ for } T_i < T_0 \tag{12}$$

4. RESULTS AND DISCUSSION

Both single- and three-column configurations, whose process schemes are reported in Figures 1 and 3, have been simulated in Aspen HYSYS V9.0.[22−25]

Each of the considered process schemes has been simulated for the inlet feed composition reported in Table 3, where the N_2

Table 3. Feed Conditions Considered for Single- and Three-Column Process Scheme Simulations

	feed flow rate	feed composition [mol fraction]			feed conditions	
case no.	[kmol/h]	CH_4	N_2	CO_2	T [°C]	P [bara]
1	1000	0.9250	0.0500	0.0250	20	50
2	1000	0.8813	0.1000	0.0187	20	50
3	1000	0.8375	0.1500	0.0125	20	50
4	1000	0.7935	0.2000	0.0065	20	50

https://dx.doi.org/10.1021/acs.iecr.0c06189
Ind. Eng. Chem. Res. 2021, 60, 4420−4429

Table 4. Conditions of Outlet Streams in Single-Column Process Scheme Simulations

			stream composition [mol fraction]			stream conditions	
stream name in Figure 1	case no	stream flow rate [kmol/h]	CH_4	N_2	CO_2	T [K]	P [bara]
upgraded natural gas	1	953.5822	0.9698	0.0040	0.0262	355.53	50.00
	2	908.6294	0.9694	0.0100	0.0206	355.53	50.00
	3	861.8052	0.9710	0.0145	0.0145	355.53	50.00
	4	819.5876	0.9671	0.0250	0.0079	355.53	50.00
N_2 vent	1	46.4178	0.005	0.995	0	278.98	27.80
	2	91.3706	0.005	0.995	0	278.98	27.80
	3	138.1948	0.005	0.995	0	278.98	27.80
	4	180.4124	0.005	0.995	0	278.98	27.80

Table 5. Conditions of Outlet Streams in Three-Column Process Scheme Simulations

			stream composition [mol fraction]			stream conditions	
stream name in Figure 3	case no	stream flow rate [kmol/h]	CH_4	N_2	CO_2	T [K]	P [bara]
CH_4_to_pipeline	1	951.0000	0.9724	0.0013	0.0263	356.76	50.00
	2	903.7997	0.9746	0.0047	0.0207	370.53	50.00
	3	856.4417	0.9770	0.0084	0.0146	380.25	50.00
	4	799.8859	0.9892	0.0027	0.0081	428.35	50.00
N_2_out	1	48.9999	0.9952	0.0048	0	278.98	1.10
	2	96.2003	0.9953	0.0047	0	278.98	1.10
	3	143.5583	0.9949	0.0041	0	278.98	1.10
	4	200.1141	0.9889	0.0011	0	278.98	1.10

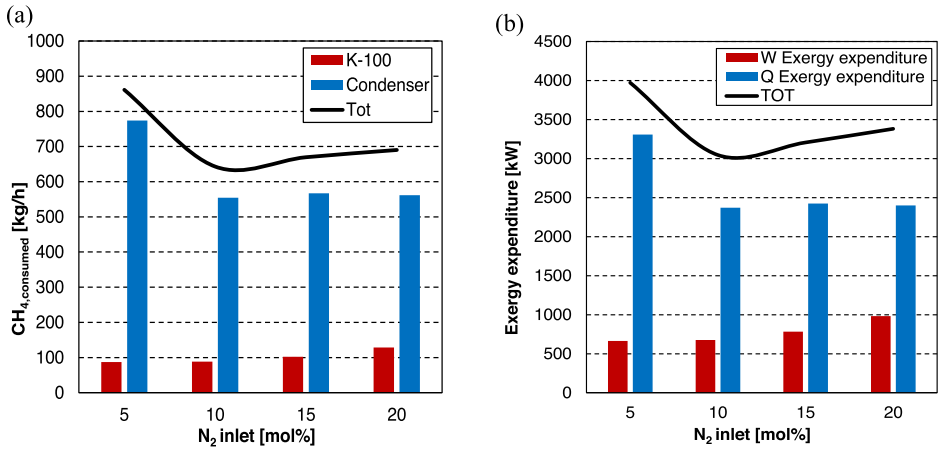

Figure 5. Single-column configuration: (a) methane consumption and (b) exergy expenditures at varying N_2 inlet contents.

molar fraction varies from 0.05 to 0.2 ($\Delta x = 0.05$) and the CO_2 content is the maximum one possible for comparing the two NRU configurations, determined thanks to the feasibility analysis reported in Figure 4 (green line in Figure 4).

Outlet streams conditions for both single- and three-column process schemes are reported in Tables 4 and 5, respectively, for each of the feed mixtures of Table 3.

For each of the simulated cases, both the equivalent methane and exergy analyses described in Section 3 have been applied in order to evaluate the process performances. In the next sections, results for the single- and three-column process schemes are reported.

4.1. Single-Column Process Scheme. The main contributions considered in both equivalent methane and exergy analyses in the single-column process scheme are the compressor K-100 and the column partial condenser.

In Figure 5, the results of both analyses are reported in terms of (a) compressor and condenser methane consumptions and (b) exergy expenditures as a function of nitrogen inlet feed composition.

With reference to Figure 5a, a minimum trend can be observed for the methane consumption associated with the column partial condenser, with a steep decrease from 5 to 10% of N_2 in the inlet feed. As a matter of fact, on increasing the N_2 content, the cooling duty required to condense the top stream decreases, decreasing the total methane flow rate inside the column. Similar conclusions result for exergy expenditures associated with the condenser, as represented in Figure 5b. On the other hand, an increasing trend results for methane consumption associated with compressor K-100. This is a consequence of the maximum allowable pressure downstream of the valve VLV_101.

https://dx.doi.org/10.1021/acs.iecr.0c06189
Ind. Eng. Chem. Res. 2021, 60, 4420−4429

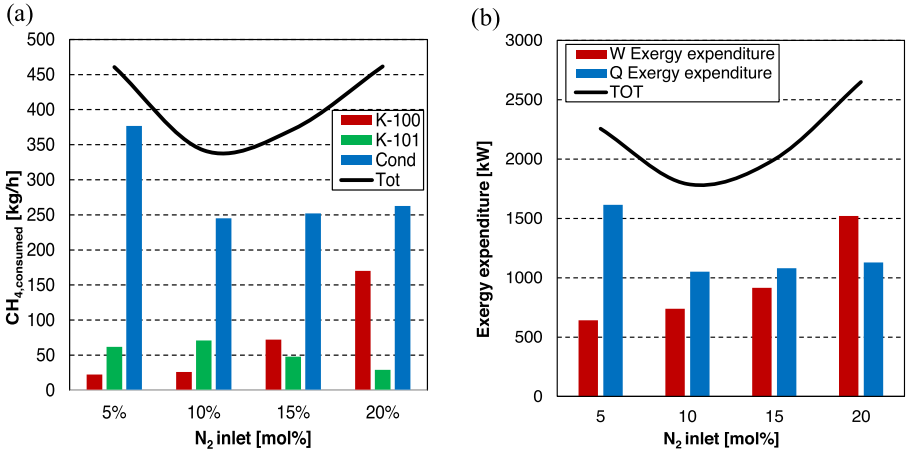

Figure 6. Three-column configuration: (a) methane consumption and (b) exergy expenditures at varying N_2 inlet contents.

The maximum allowable expansion performed by the valve is limited by CO_2 solidification. On increasing the N_2 inlet content, the CO_2 inlet content decreases in order to avoid solidification issues within the plant. As the CO_2 content in the bottom product decreases with increasing the N_2 content, the distillation column residue CH_4 product can be expanded at lower pressures to perform heat integration in the LNG-100 heat exchanger. On increasing the nitrogen inlet content, lower pressures and thus lower temperatures are required to make the thermal coupling feasible in LNG-100, the bottom product flow rate being lower. For this reason, recompression work in K-100 is higher on increasing the N_2 inlet content.

As a result of both methane-equivalent and exergy analyses, the total energy and exergy expenditures as a function of the inlet N_2 concentration for the single-column process scheme show a minimum located around 10 mol % N_2, suggesting that the best process performances are registered in this case.

4.2. Three-Column Process Scheme. The main contributions associated with both methane-equivalent and exergy analyses in the three-column process scheme are the compressors K-100 and K-101 and the preseparation column partial condenser. As stated in Section 2.1, the double-column process is autothermal and so it has not been considered in the following analysis.

Similar to the single-column configuration, the results of the equivalent methane and exergy analyses are reported in Figure 6.

With reference to Figure 6a, the equivalent methane consumption associated with the preseparation column partial condenser shows a minimum trend, as seen in the single-column case. Similar results are obtained in terms of the preseparation column partial condenser exergy expenditures, as depicted in Figure 6b.

On the other hand, energy and exergy consumptions of K-100 and K-101 compressors show opposite trends: while K-100 compression work increases on increasing the N_2 inlet content, K-101 decreases (except for 5 and 10 mol % N_2, where the higher methane purity causes an increase in the compressor power demand). This can be understood considering that K-100 is the double-column product compressor, whereas K-101 is the preseparation column one. On increasing the N_2 inlet content, the top product flow rate of the preseparation column, i.e., the flow rate that must be treated by the downstream double column, increases. On the contrary, the bottom product flow rate of the preseparation column decreases.

4.3. Comparison between Single-Column and Three-Column Process Schemes. Referring to the total CH_4 consumption reported in Figure 5, the equivalent methane per mole of inlet methane is reported in Figure 7.

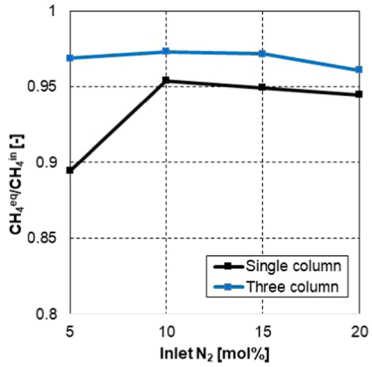

Figure 7. Equivalent methane of single- and three-column nitrogen rejection schemes.

As a matter of fact, the closer the equivalent methane per mole of inlet methane to 1, the less is the energy consumed. As expected, the three-column process scheme is always less energy-intensive than the single-column scheme for each of the analyzed inlet feed compositions. The resulting equivalent methane for the three-column configuration is almost constant and close to 1, meaning that few methane-consuming processes are associated with the three-column configuration. On the other hand, the single-column process scheme shows a less constant trend, this configuration being more dependent on the inlet N_2 feed content.

The difference between the two process configurations is maximum for the inlet feed compositions containing 5 mol % N_2 and decreases as the nitrogen feed content increases. This result suggests that, for high nitrogen feed content, a capital expense estimate is needed to verify if the higher three-column process scheme complexity (thus, higher fixed costs) can be justified by the energy savings depicted (thus, lower operating costs).

Proving that the three-column configuration is more energy-efficient and is capable of guaranteeing higher equivalent methane production, the exergy efficiency associated with both process schemes has been analyzed and reported in Figure 8.

https://dx.doi.org/10.1021/acs.iecr.0c06189
Ind. Eng. Chem. Res. 2021, 60, 4420−4429

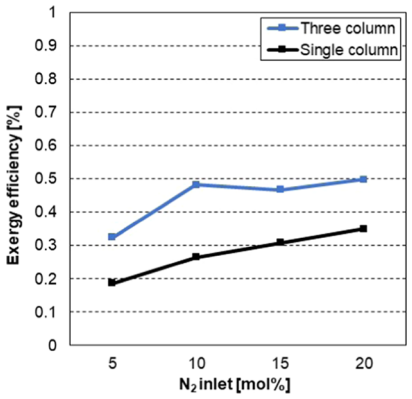

Figure 8. Exergy efficiency of single- and three-column nitrogen rejection schemes.

Exergy efficiency associated with both single- and three-column process schemes ranges from around 0.3 to 0.5. Thus, the efficiency of this plant is quite low, which means that there are large irreversibilities associated with processes occurring in the compressors and the condensers.

Nevertheless, these values have been compared with those for the cryogenic air separation process, which also involves low-pressure N_2. As the exergy efficiency associated with Linde N_2−O_2 fractionation η_{ex} = 0.36,[26] the nitrogen rejection exergy efficiency appears in line with the one related to the cryogenic air separation. In nitrogen rejection configurations, a very high exergy expenditure is associated with the condenser in both single- and three-column process schemes. A separate exergy analysis on this equipment can provide, in principle, suggestions for process optimization. The exergy efficiencies of both single- and three-column process schemes show a quite increasing trend with the nitrogen feed inlet content, with the three-column process scheme being more exergy-efficient than that of the single column for each of the cases analyzed.

To better understand the exergy flows that cross system boundaries, Grassmann diagrams have been reported in Figures 9 and 10 for the two analyzed process configurations at varying inlet feeds: gray arrows represent the exergy associated with material streams, while black arrows represent the exergy equivalents of heat and work flows.

With reference to Figures 9 and 10, the numerical differences between all of the inlet and outlet flows of the two schemes result in the total exergy destructions caused by the systems. As can be inferred from the numerical results collected in Table 6, the exergy destructions decrease with increasing nitrogen content; the system is more efficient with the three-column configuration and shows the minimum difference between inlet and outlet streams for 10 mol % N_2.

5. CONCLUSIONS

Process selection for the NRU should be based on operating flexibility, the complexity of the process scheme, and sensitivity to feed gas compositions in addition to life cycle costs. The key parameters for process selection are the feed gas nitrogen and CO_2 contents, feed pressure, flow rate, methane recovery, and contaminant level.

Following a previous feasibility study[4] for different NRU schemes in the presence of CO_2, this work investigates the

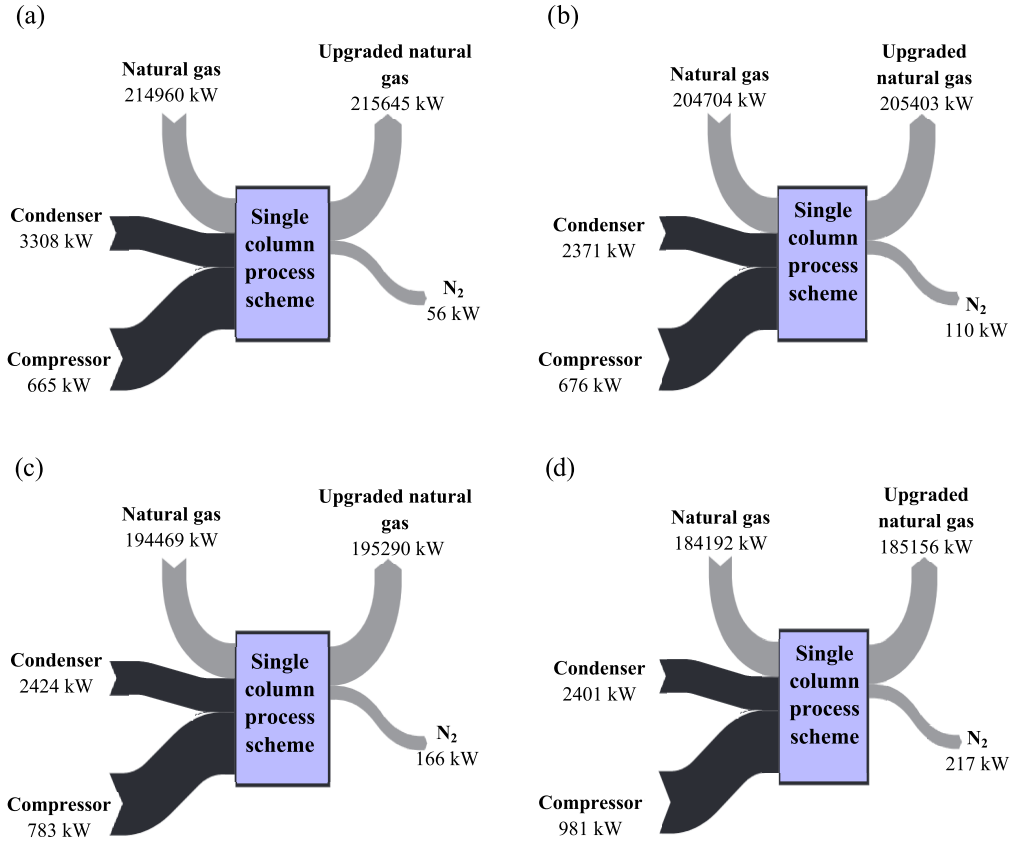

Figure 9. Grassmann diagram for the single-column process scheme for inlet N_2 of (a) 5 mol %, (b) 10 mol %, (c) 15 mol %, and (d) 20 mol %.

https://dx.doi.org/10.1021/acs.iecr.0c06189
Ind. Eng. Chem. Res. 2021, 60, 4420−4429

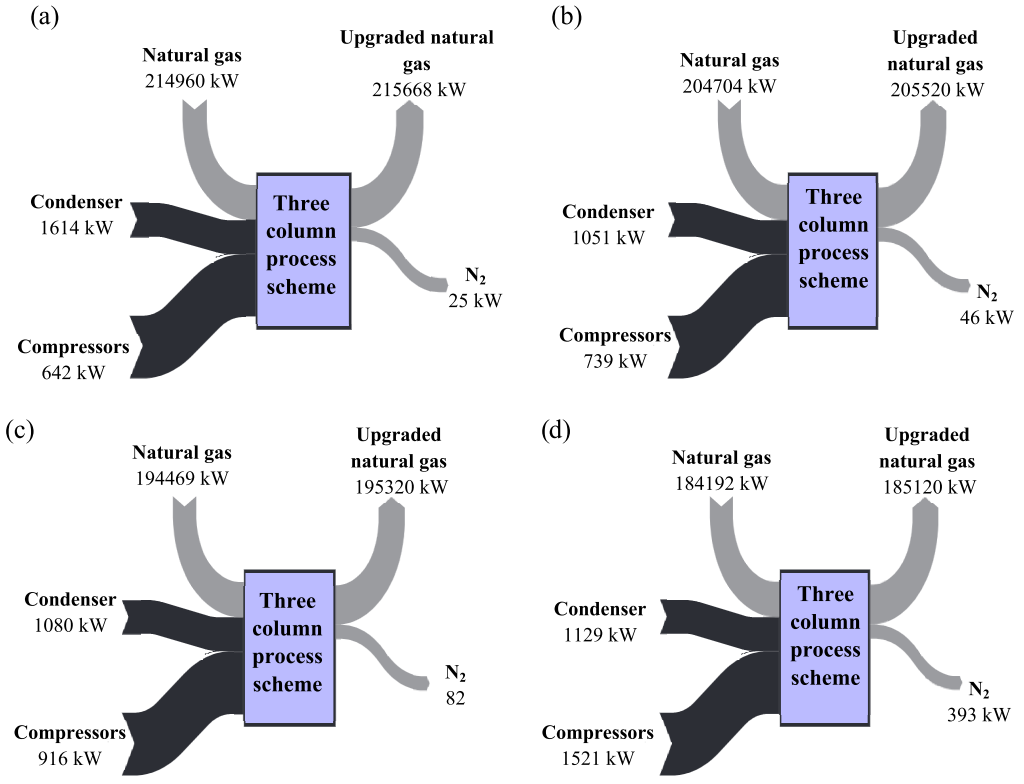

Figure 10. Grassmann diagram for the three-column process scheme for inlet N_2 of (a) 5 mol %, (b) 10 mol %, (c) 15 mol %, and (d) 20 mol %.

Table 6. Total Exergy Destructions for Single- and Three-Column Process Schemes

	exergy destructions [kW]	
inlet N_2 [mol %]	single column	three column
5	3231.76	1524.16
10	2238.27	927.09
15	2220.30	1062.59
20	2200.96	1329.25

process energy and exergy performances by means of the equivalent methane and exergy analyses.

While energy analysis provides absolute values for the methane required to sustain each process, exergy analysis provides a value for their efficiencies, enabling us to quantify how much each process is far from the ideal thermodynamic reference process. Therefore, even if the thermodynamic performance ranking of the three analyzed processes is the same according to energy and exergy analyses, the latter provides more useful information and thus it is preferred.

This paper demonstrates that the three-column process scheme configuration for nitrogen rejection from natural gas provides the most convenient configuration in terms of energy and exergy expenditures, if compared to the other available process schemes.

The higher complexity of the three-column process scheme is balanced not only by its higher energy and exergy performances, but also by its higher flexibility in terms of CO_2 feed content compared to the single-column process, thus requiring a not too deep CO_2 removal upstream.

AUTHOR INFORMATION

Corresponding Author

Elvira Spatolisano − *Dipartimento di Chimica, Materiali e Ingegneria Chimica "G. Natta", Politecnico di Milano, 20133 Milano, Italy;* orcid.org/0000-0002-3316-0487; Phone: +39 02 2399 3207; Email: elvira.spatolisano@polimi.it; Fax: +39 02 2399 3280

Author

Laura A. Pellegrini − *Dipartimento di Chimica, Materiali e Ingegneria Chimica "G. Natta", Politecnico di Milano, 20133 Milano, Italy*

Complete contact information is available at: https://pubs.acs.org/10.1021/acs.iecr.0c06189

Notes

The authors declare no competing financial interest.

ABBREVIATIONS

COP coefficient of performance
IEA International Energy Agency
LHV lower heating value
LNG liquefied natural gas
NRU nitrogen rejection unit
WI Wobbe index

Greek Symbols

η efficiency
τ_i Carnot factor associated to mixture i

REFERENCES

(1) Just Evolution 2030. The Socio-Economic Impacts of Energy Transition in Europe. In *The European House—Ambrosetti for Enel and Enel Foundation*; Grafica Internazionale: Roma, 2019.

https://dx.doi.org/10.1021/acs.iecr.0c06189
Ind. Eng. Chem. Res. 2021, 60, 4420−4429

(2) Janoska, P. Energy Transitions Indicators. In *Tracking Energy Transitions*; International Energy Agency (IEA), 2019.
(3) World Energy Model. *Scenario Analysis of Future Energy Trends*; IEA, Energy Outlook, 2020.
(4) De Guido, G.; Messinetti, F.; Spatolisano, E. Cryogenic Nitrogen Rejection Schemes: Analysis of Their Tolerance to CO_2. *Ind. Eng. Chem. Res.* **2019**, *58*, 17475−17488.
(5) The Linde Group State-of-the-art nitrogen rejection technology-Increasing the energy density of natural gas , 2019.
(6) Kidnay, A. J.; Parrish, W. R., *Fundamentals of Natural Gas Processing*; CRC Press Taylor & Franscis Group: Boca Raton, FL, USA, 2006.
(7) *Aspen HYSYS*; AspenTech: Burlington, MA, USA, 2016.
(8) MacKenzie, D.; Cheta, I.; Burns, D. Removing Nitrogen. In *Hydrocarbon Engineering*; Palladian Publications, 2002; Vol. 7, pp 57−63.
(9) Ott, C. M.; Roberts, M. J.; Trautmann, S. R.; Krishnamurthy, G. State-of-the-Art Nitrogen Removal Methods from Air Products for Liquefaction Plants, 2015. http://www.airproducts.com/~/media/Files/PDF/industries/lng/en-LNG-journal-paper.pdf.
(10) Rufford, T. E.; Smart, S.; Watson, G. C.; Graham, B.; Boxall, J.; Da Costa, J. D.; May, E. The removal of CO_2 and N_2 from natural gas: A review of conventional and emerging process technologies. *J. Pet. Sci. Eng.* **2012**, *94*−*95*, 123−154.
(11) Johnson, G. L.; Finn, A. J.; Tomlinson, T. R. Process and Apparatus for Separation of Hydrocarbons and Nitrogen. U.S. Patent US13/259,3552012.
(12) Johnson, G. L.; Tomlinson, T. R.; Phillips, L. A. Process and Apparatus for Separation of Hydrocarbons and Nitrogen. U.S. Patent US13/259,3552012.
(13) Johnson, G. L.; Finn, A. J. Process and Apparatus for Separation of Hydrocarbons and Nitrogen. U.S. Patent US13/259,3552016.
(14) Mokhatab, S.; Mak, J.; Valappil, J.; Wood, D. *Handbook of Liquefied Natural Gas*; Gulf Professional Publishing: Book Division, Houston, TX, 2013.
(15) De Guido, G.; Fogli, M. R.; Pellegrini, L. A. Effect of Heavy Hydrocarbons on CO_2 Removal from Natural Gas by Low-Temperature Distillation. *Ind. Eng. Chem. Res.* **2018**, *57*, 7245−7256.
(16) Pellegrini, L. A.; De Guido, G.; Lodi, G.; Mokhatab, S. CO_2 Capture from Natural Gas in LNG Production—Comparison of Low-Temperature Purification Processes and Conventional Amine Scrubbing. In *Cutting-Edge Technology for Carbon Capture, Utilization, and Storage*; Ballerat-Busserolles, K.; Wu, Y.; Carroll, J. J., Eds.; Wiley, 2018; p 384.
(17) Kotas, T. J. *The Exergy Method of Thermal Plant Analysis*; Elsevier: Paragon, 2012.
(18) Bejan, A. *Advanced Engineering Thermodynamics*; John Wiley & Sons, 2006.
(19) Kotas, T. J. *The Exergy Method of Thermal Plant Analysis*; Malabar Elsevier, 2013.
(20) Bejan, A.; Tsatsaronis, G.; Moran, M. *Thermal Design and Optimization*, 1st ed.; John Wiley & Sons: New York, 1996.
(21) Baccanelli, M.; Langé, S.; Rocco, M. V.; Pellegrini, L. A.; Colombo, E. Low temperature techniques for natural gas purification and LNG production: an energy and exergy analysis. *Appl. Energy* **2016**, *180*, 546−559.
(22) Kuo, J.; Wang, K.; Chen, C. Pros and cons of different Nitrogen Removal Unit (NRU) technology. *J. Nat. Gas Sci. Eng.* **2012**, *7*, 52−59.
(23) Kohl, A. L.; Nielsen, R. *Gas Purification*; Gulf Professional Publishing: Houston, TX, USA, 1997.
(24) Farooq, A.; Finn, A.; Hosainy, A.; Johnson, G. In *Carbon Dioxide-Tolerant Nitrogen Rejection Reduces Costs*, GPA Europe Annual Conference, Florence, Italy, 2015.
(25) Eggeman, T.; Chafin, S. In *Pitfalls of CO_2 Freezing Prediction*, Proceedings of the 82nd Annual Convention of the Gas Processors Association, San Antonio, TX, USA, 2003.
(26) Hamdy, S.; Moser, F.; Morosuk, T.; Tsatsaronis, G. Exergy-Based and Economic Evaluation of Liquefaction Processes for Cryogenics Energy Storage. *Energies* **2019**, *12*, No. 493.

https://dx.doi.org/10.1021/acs.iecr.0c06189
Ind. Eng. Chem. Res. 2021, 60, 4420−4429